

# (Very) Stable Boundary Layers – An Introduction



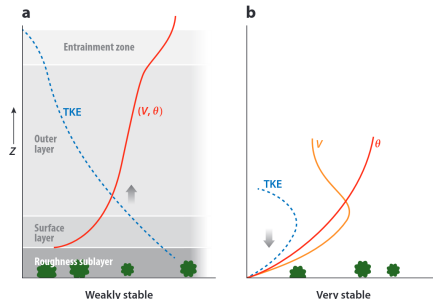
# Stable Boundary Layer (SBL) Regimes

## weakly stable (wSBL)

- ▶ sublayer, surface layer, outer layer
  - ▶ turbulence balances radiative cooling
- atmosphere and surface are *coupled*

## very stable (vSBL)

- ▶ very shallow surface layer
  - ▶ turbulence can't balance radiative cooling (higher  $Ri$ )
- atmosphere and surface are *decoupled*

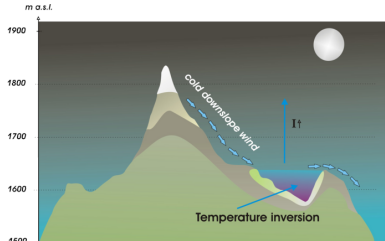


(Mahrt, 2014)

# SBL Formation and Interaction with Orography

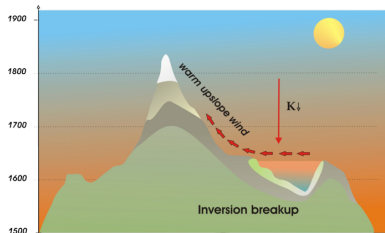
## synoptic-scale

- ▶ subsidence
- ▶ clear sky
- ▶ calm
- ▶ most favorable: high pressure system during (polar) night/winter



## orography-induced

- ▶ cold-air drainage
- ▶ katabatic flows
- ▶ cold-air pools



(katabatic/anabatic flows, wikipedia)

# SBL Processes | submeso-scale motions, intermittency

**submeso-scale motions:** (gravity) waves, meandering, solitons, microfronts, ...

- ▶ wave-turbulence interaction
- ▶ intermittency
- ▶ strong sensitivity to surface characteristics



(pictures: [submeso.org](http://submeso.org))

# SBL Theory | TKE equation and MOST

**TKE tendency equation** (simplified for surface layer):

$$\frac{\partial}{\partial t} TKE = \overline{u'w'} \frac{\partial \bar{U}}{\partial z} + \frac{g}{\theta} \overline{w'\theta'} + T - \epsilon$$

**mechanical production:** strong shear under stable conditions

**buoyancy production:** negative (i.e. sink) under stable conditions

transport/divergence (neglected for MOST)

dissipation

# SBL Theory | TKE equation and MOST

**TKE tendency equation** (simplified for surface layer):

$$\frac{\partial}{\partial t} TKE = \overline{u'w'} \frac{\partial \bar{U}}{\partial z} + \frac{g}{\theta} \overline{w'\theta'} + T - \epsilon$$

**mechanical production:** strong shear under stable conditions

**buoyancy production:** negative (i.e. sink) under stable conditions

transport/divergence (neglected for MOST)

dissipation

**Monin-Obukhov similarity theory** (Monin and Obukhov, 1954)

→ log-linear wind profiles

$$U(z) = \frac{u_*}{\kappa z} \Phi_m(Ri)$$

with  $\Phi_m(Ri)$ : stability correction function (derived from observations)

assumptions: flat and homogeneous surface, steady flow

# SBL Theory | TPE equation and EFB

**TKE tendency equation** (simplified for surface layer):

$$\frac{\partial}{\partial t} TKE = \overline{u'w'} \frac{\partial \bar{U}}{\partial z} + \frac{g}{\bar{\theta}} \overline{w'\theta'} + T_K - \epsilon_K$$

# SBL Theory | TPE equation and EFB

**TKE tendency equation** (simplified for surface layer):

$$\frac{\partial}{\partial t} TKE = \overline{u'w'} \frac{\partial \bar{U}}{\partial z} + \frac{g}{\bar{\theta}} \overline{w'\theta'} + T_K - \epsilon_K$$

**TPE tendency equation** (simplified for surface layer):

$$\frac{\partial}{\partial t} TPE = -\frac{g}{\bar{\theta}} \overline{w'\theta'} + T_P - \epsilon_P$$

$$\text{turbulent potential energy } TPE = \left( \frac{g}{\bar{\theta} N} \right)^2 \overline{\theta'^2}$$

**Energy-Flux Budget (EFB) closure** (Zilitinkevich et al., 2008/2013)

- considering total turbulent energy  $TTE = TKE + TPE$
- sensible heat flux cancels out
- turbulence can be maintained above critical Richardson number

# Studying SBLs

## modelling

- ▶ Reynolds-averaged Navier-Stokes (RANS) equation (numerical weather prediction (NWP) / climate models)
- ▶ large-eddy simulations (LES)
- ▶ direct numerical simulations (DNS)
- ▶ idealized numerical studies

## observations

- ▶ eddy-covariance measurements
- ▶ fiber-optic distributed sensing
- ▶ remote sensing: wind lidar, sodar, microwave radiometer
- ▶ drones

# **Example 1:**

## Validating NWP models with fiber-optic distributed sensing

# Fieldwork | Overview

## Measurement setup:

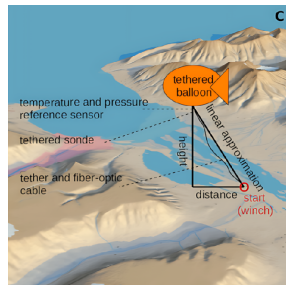
- ▶ flight1 (28.01.2024): weak synoptic forcing
- ▶ flight2 (01.02.2024): strong synoptic forcing
- ▶ ancillary:  
tether sonde, reference sensor @ balloon height,  
eddy-covariance measurements @ weather station



## Fiber-Optic Distributed Sensing (FODS):

- ▶ high-resolution temperature profiles  
(25 cm, 10 s)
- ▶ relatively recently established (Thomas et al., 2012)
- ▶ used for: submeso motions and fronts, cold air layers, morning transitions (e.g. Pfister et al., 2021a,b)

→ **our study:** Airborne FODS in Arctic and model verification

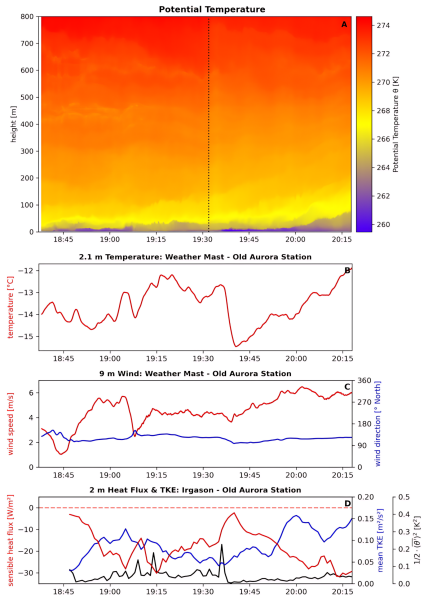


(toposvalbard.no)

# Fieldwork | Overview



# Results | Flight1 (28.01.2024): Weak synoptic forcing



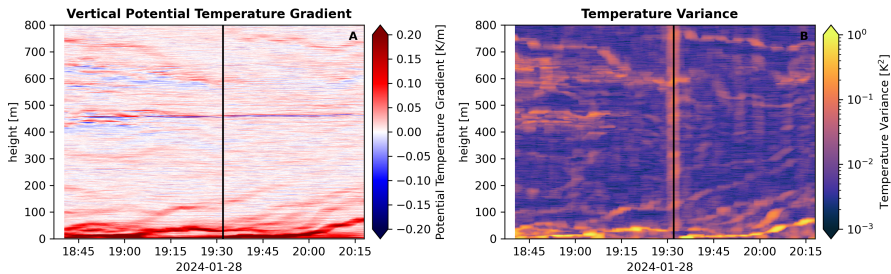
▷ FODS-derived potential temperature

▷ weather station measurements  
(temperature, wind speed, wind direction)

▷ eddy-covariance measurements  
(sensible heat flux, TKE, TPE)

# Results | Flight1 (28.01.2024): Weak synoptic forcing

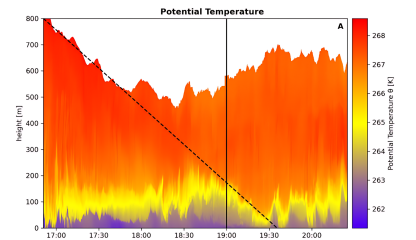
- ▶ potential temperature gradient and temperature variance



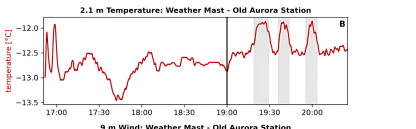
## Observations Flight1:

- ▶ "classical" stable conditions: surface-based inversion and elevated valley inversions

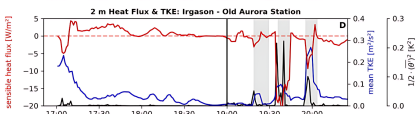
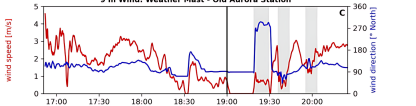
# Results | Flight2 (01.02.2024): Strong synoptic forcing



▷ FODS-derived potential temperature



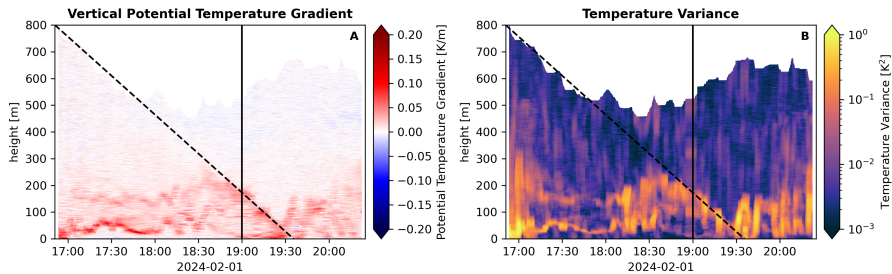
▷ weather station measurements  
(temperature, wind speed, wind direction)



▷ eddy-covariance measurements  
(sensible heat flux, TKE, TPE)

# Results | Flight2 (01.02.2024): Strong synoptic forcing

- ▶ potential temperature gradient and temperature variance



## Observations Flight2:

- ▶ changing background flow: weaker surface-based inversion and warm front passage

# Model verification | Overview

## AROME-Arctic (AA25) (operational):

(Müller et al., 2017)

- ▶ horizontal resolution: 2.5 km
- ▶ lowest model levels: 12 m, 36 m, 60 m

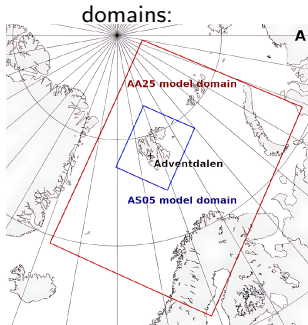
## AROME-Svalbard (AS05) (experimental):

(Valkonen et al., 2020)

- ▶ horizontal resolution: 0.5 km
- ▶ lowest model levels: 5 m, 15 m, 29 m
- ▶ updated snow scheme, physiography, differences in domain, BC, DA, ...

**runs:** main cycle (00 UTC), hourly output

**initialization:** AS05: 22.01.2024 03 UTC



grids: AA25



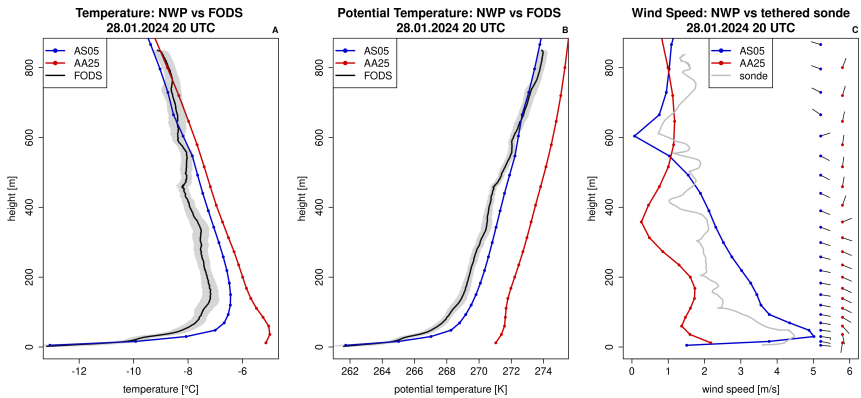
AS05



(toposvalbard.no)

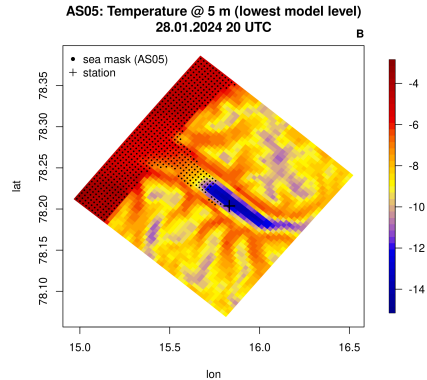
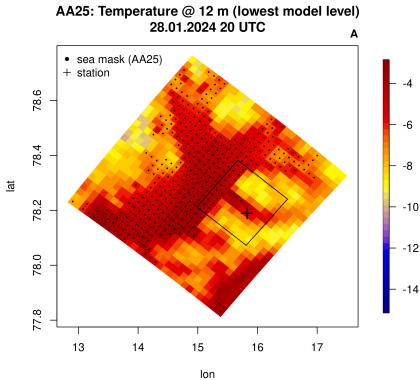
# Results | Flight1 (28.01.2024): Weak synoptic forcing

- ▶ vertical profiles of (potential) temperature and wind speed: obs vs model



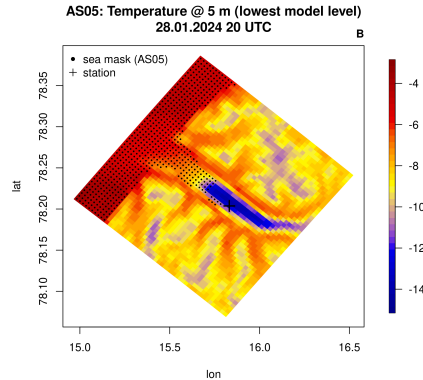
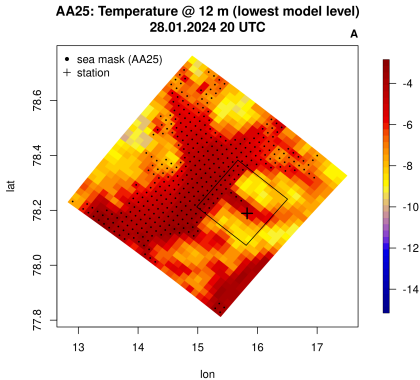
# Results | Flight1 (28.01.2024): Weak synoptic forcing

- temperature @ first model level



# Results | Flight1 (28.01.2024): Weak synoptic forcing

- temperature @ first model level

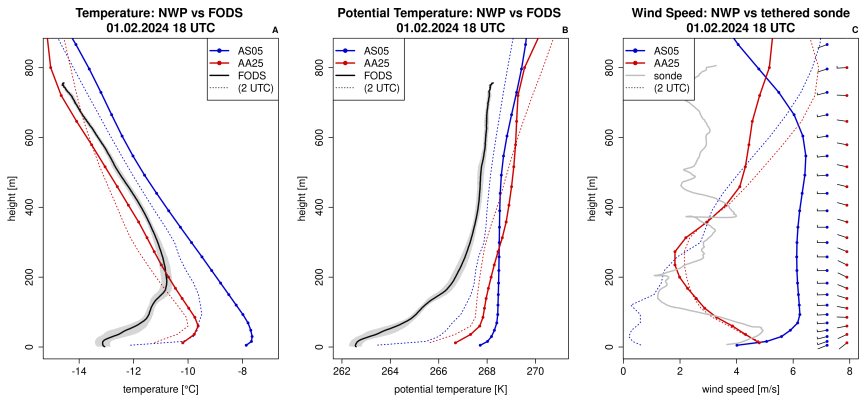


## Results Flight 1:

- AS05: representation of inherent stable boundary layer features (cold pool and LLJ)  
→ well-represented vertical temperature profile
- AA25: stable boundary layer features not represented → warm bias

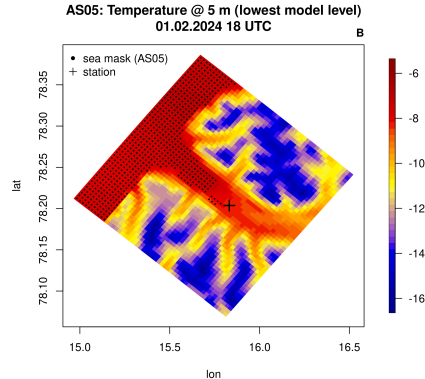
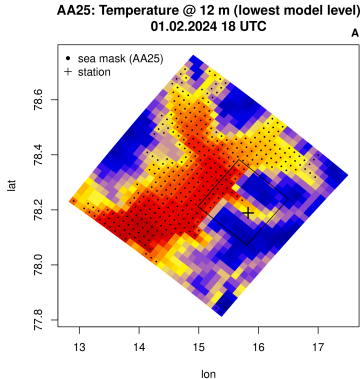
# Results | Flight2 (01.02.2024): Strong synoptic forcing

- ▶ vertical profiles of (potential) temperature and wind speed: obs vs model



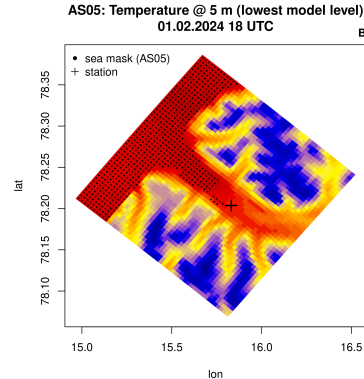
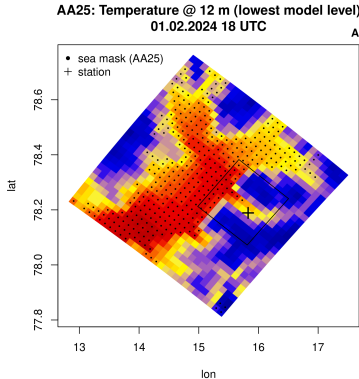
# Results | Flight2 (01.02.2024): Strong synoptic forcing

- ▶ vertical profiles of (potential) temperature and wind speed: obs vs model



# Results | Flight2 (01.02.2024): Strong synoptic forcing

- ▶ vertical profiles of (potential) temperature and wind speed: obs vs model



## Results Flight 2:

- ▶ AS05: valley inflow and valley channeling → warm air advection from fjord → warm bias
- ▶ AA25: valley inflow, but no valley channeling → weaker warm air advection

# Summary | FODS for model verification

## model verification:

- ▶ "classical" stable conditions: **hectometric-scale model** represents stable boundary layer features → outperforms **kilometer-scale model**
- ▶ changing background flow: **hectometric-scale model** more sensitive to misrepresented mesoscale wind direction → **kilometer-scale model** seemingly better agreement with observations

## model and topography resolution:

- ▶ ratio model resolution versus valley width  $\Delta x/L$  determines model's ability to represent orographically caused flows → threshold  $\Delta x/L \approx 0.1$  (Wagner et al., 2014)
  - here: Adventdalen (width  $L = 4$  km)
  - AS05**:  $\Delta x = 0.5$  km →  $\Delta x/L = 0.125$
  - AA25**:  $\Delta x = 2.5$  km →  $\Delta x/L = 0.625$
- ▶ low lowest model level determines model's ability to represent strong surface-based temperature inversions and low-level jets adequately

## Example 2:

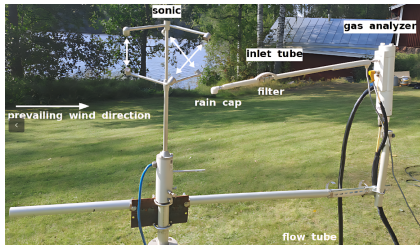
Eddy-covariance measurements for SBL studies



# Eddy-covariance measurements

## Setup

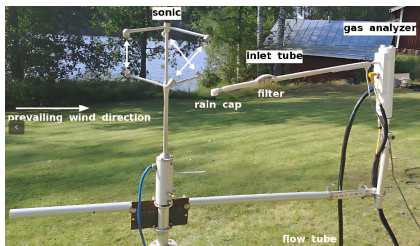
- ▶ sonic:  $u$ ,  $v$ ,  $w$ ,  $T$
- ▶ gas analyzer:  $H_2O$ ,  $CO_2$ ,  $CH_4$ ,  $NO$ , particles
- ▶ high sampling frequency (e.g. 20 Hz)



# Eddy-covariance measurements

## Setup

- ▶ sonic:  $u, v, w, T$
- ▶ gas analyzer:  $H_2O, CO_2, CH_4, NO$ , particles
- ▶ high sampling frequency (e.g. 20 Hz)



## Eddy-covariance method

- ▶ Reynolds averaging:

$$x = \bar{x} + x', \quad \bar{x} := \frac{1}{t_s} \int_0^{t_s} x \, dt$$

- ▶ flux calculation:

$$\begin{aligned}\overline{xy} &= \bar{x} \bar{w} + \bar{x} \overline{w'} + \overline{x'} \bar{w} + \overline{x'} \overline{w'} \\ &= \bar{x} \bar{w} + \overline{x' w'}\end{aligned}$$

usually:

$w$ : vertical velocity

$x$ : scalar

$\overline{x' w'}$ : vertical flux of  $x$

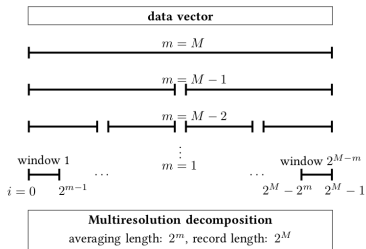
- ▶ a lot of post-processing
- ▶ How to determine the averaging time?

# Methods: Multiresolution Decomposition (MRD)

## Multiresolution Decomposition (MRD)

(Vickers & Mahrt, 2002)

- ▶ spectrum/cospectrum (starting with high-frequency timeseries)
- ▶ wavelet decomposition (Haar wavelets)
- ▶ averaging time:  
stable: 1-10 min  
unstable: 30 min



# Methods: Anisotropy Analysis

## Reynolds stress tensor

$$\begin{aligned} R &= \overline{u'_i u'_j} \\ &= \begin{pmatrix} \overline{u'^2} & \overline{u' v'} & \overline{u' w'} \\ \overline{v' u'} & \overline{v'^2} & \overline{v' w'} \\ \overline{w' u'} & \overline{w' v'} & \overline{w'^2} \end{pmatrix} \end{aligned}$$

- ▶ invariant analysis (eigenvalues)
- ▶ projection in 2d map

**velocity aspect ratio:**  $VAR = \frac{\overline{w'^2}}{\overline{u'^2} + \overline{v'^2}}$

- ▶ measure for isotropy
- ▶ but: cannot distinguish 1- and 2-component

# Methods: Anisotropy Analysis

## Reynolds stress tensor

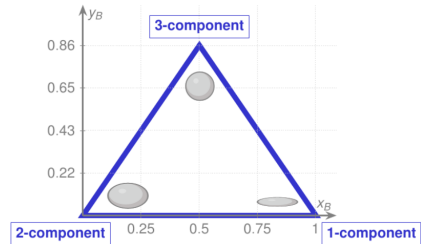
$$\begin{aligned} R &= \overline{u'_i u'_j} \\ &= \begin{pmatrix} \overline{u'^2} & \overline{u' v'} & \overline{u' w'} \\ \overline{v' u'} & \overline{v'^2} & \overline{v' w'} \\ \overline{w' u'} & \overline{w' v'} & \overline{w'^2} \end{pmatrix} \end{aligned}$$

- ▶ invariant analysis (eigenvalues)
- ▶ projection in 2d map

**velocity aspect ratio:**  $VAR = \frac{\overline{w'^2}}{\overline{u'^2} + \overline{v'^2}}$

- ▶ measure for isotropy
- ▶ but: cannot distinguish 1- and 2-component

## Barycentric map



$y_B$ : anisotropy

3-component: spherical (isotropic)

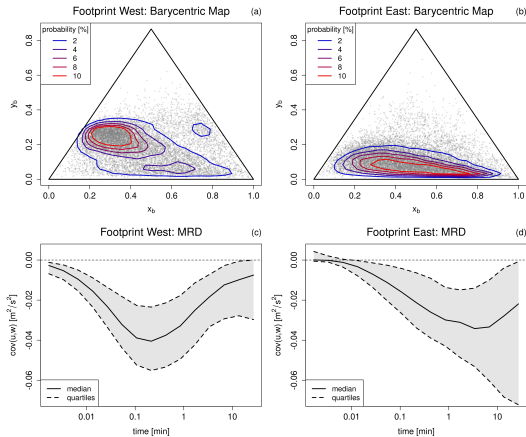
2-component: disk-like (sheared)

1-component: rod-like (waves)

# Example: Finse

## footprint-dependent MRD and anisotropy analysis

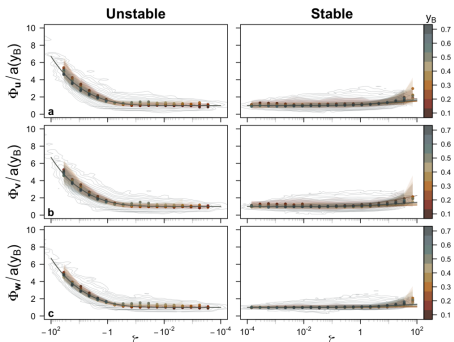
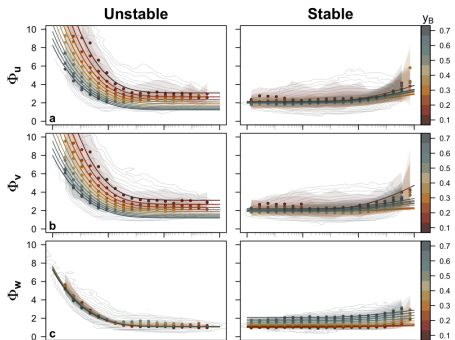
- ▶ west: shear-driven anisotropic turbulence (2-component)
- ▶ east: wave-dominated, submeso-scale (towards 1-component)



# Example: MOST scaling with anisotropy

## MOST with anisotropy

- anisotropy explains (parts of) scatter around scaling functions



(Stiperski, 2022)

# Summary and Outlook

## Summary:

- ▶ regimes: weakly vs. very stable
- ▶ phenomena under very stable stratification: waves, intermittency
- ▶ classical turbulence parameterizations fail → problem in NWP

## Outlook:

- ▶ spatial analysis
- ▶ statistical/stochastical modelling

## Links to studies

**example 1:** <https://agupubs.onlinelibrary.wiley.com/doi/full/10.1029/2024JD042825>  
**example 2:** <https://link.springer.com/article/10.1007/s10546-024-00879-5>